NAVAL SHIP RESEARCH AND DEVELOPMENT CENTER
WASHINGTON, D.C. 20007

OSCILLATION OF CYLINDERS IN OR BELOW THE FREE SURFACE OF DEEP FLUIDS

HYDROMECHANICS LABORATORY
RESEARCH AND DEVELOPMENT REPORT

October 1967

Report 2375

OSCILLATION OF CYLINDERS IN OR BELOW THE FREE SURFACE OF DEEP FLUIDS

by

W. Frank

ABSTRACT

The subject of cylinders oscillating in or below the free surface of very deep fluids is developed as a boundary value problem within the framework of linear free-surface theory by distributing source singularities over the submerged portion of the cylinders. A computer program for calculating the hydrodynamic pressure, force, and moment on these cylinders has been devised by the Naval Ship Research and Development Center. The results for various two-dimensional shapes are given in graphical form.

ADMINISTRATIVE INFORMATION

This study was authorized by the Naval Ship Systems Command under the General Hydromechanics Research Program, and it was funded under Subproject S-R009 01 01, Task 0100.

TABLE OF CONTENTS

LIST OF FIGURES

NOTATION

$A^{(m)}$	Oscillation amplitude in the m th mode
B	Beam of cross section C_0
C_0	Submerged part of cross sectional contour in rest position
g	Acceleration due to gravity
$I_{ij}^{(m)}$	Influence coefficient in phase with displacement on the ith midpoint due to the jth segment in the m th mode of motion
$J_{ij}^{(m)}$	Influence coefficient in phase with velocity on the ith midpoint due to the jth segment in the m th mode of oscillation
$M_{(\omega)}^{(m)}$	Added mass force or moment for the m th mode of oscillation at frequency ω
N	Number of line segments defining submerged portion of half section in rest position
$N_{(\omega)}^{(m)}$	Damping force or moment for the m th mode of oscillation at frequency ω
$n_i^{(m)}$	Direction cosine of the normal velocity at ith midpoint for mth mode of oscillation
$P.V.$	Cauchy principal value of integral
$p_a^{(m)}$	Hydrodynamic pressure in phase with displacement for m th mode of oscillation
$p_v^{(m)}$	Hydrodynamic pressure in phase with velocity for m th mode of oscillation
$Q_j^{(m)}$	Source strength in phase with displacement along jth segment for m th mode of oscillation
$Q_{j+N}^{(m)}$	Source strength in phase with velocity along jth segment for m th mode of oscillation
s	Length variable along C_0
s_j	jth line segment
T	Draft of cross section

t	Time
$v_i^{(m)}$	Normal velocity component at ith midpoint for mth mode of oscillation
x_i	Abscissa of ith midpoint
y_i	Ordinate of ith midpoint
y_0	Ordinate of center of roll
s	Complex field point in region of fluid domain ($s = x + iy$)
s_i	Complex midpoint of ith segment ($s_i = x_i + iy_i$)
α_i	Angle between ith segment and positive x axis
ζ	Complex variable along C_0
ζ_j	jth complex input point along C_0
η_j	Ordinate of jth input point
ν	Wave number ($= \omega^2/g$)
ν_k	kth irregular wave number for adjoint interior problem
ξ_j	Abscissa of jth input point
ρ	Density of fluid
$\Phi^{(m)}$	Velocity potential for mth mode of oscillation
ω	Radian frequency of oscillation
ω_k	kth irregular frequency for adjoint interior problem (kth eigenfrequency)

INTRODUCTION

Hydrodynamic research of horizontal cylinders oscillating in or below the free surface of a deep fluid has increased in importance in the past two decades and has been studied by a number of investigators. The modern history of this subject began with Ursell,[1] who formulated and solved the boundary-value problem for the semi-immersed heaving circular cylinder within the framework of linearized free-surface theory. He represented the velocity potential as the sum of an infinite set of multipoles, each satisfying the linear free-surface condition and each being multiplied by a coefficient determined by requiring the series to satisfy the kinematic boundary condition at a number of points on the cylinder.

Grim[2] used a variation of the Ursell method to solve the problem for two-parameter, Lewis-form cylinders by conformal mapping onto a circle. Tasai[3] and Porter,[4] using the Ursell approach, obtained the added mass and damping for oscillating contours mappable onto a circle by the more general Theodorsen transformation. At the Naval Ship Research and Development Center, Ogilvie[5] calculated the hydrodynamic forces on completely submerged heaving circular cylinders.

Despite the success of the multipole expansion-mapping methods, the present paper discusses the problem from a different view. The velocity potential is represented by a distribution of sources over the submerged cross section. The density of the sources is an unknown function (of position along the contour) to be determined from integral equations found by applying the kinematic boundary condition on the submerged part of the cylinder. The hydrodynamic pressures are obtained from the velocity potential by means of the linearized Bernoulli equation. Integration of these pressures over the immersed portion of the cylinder yields the hydrodynamic forces or moments.

A simpler approximation to the solution of the two-dimensional hydrodynamic problem was used in the strip theory of ship motions introduced by Korvin-Kroukovsky.[6] The solutions of two-dimensional, water-wave problems for ship sections by multipole expansion and mapping techniques have been applied to this strip theory by Gerritsma,[7] Smith,[8] Grim,[9] and Vassilopoulos[10] to predict the heaving and pitching motions of surface vessels moving in

---

[1] References are listed on page 39.

head or following seas. This report has largely been motivated by the desirability of devising a computer program, based on strip theory and independent of mapping techniques, to predict the response of surface ships moving with steady forward speed in oblique as well as head or following seas for all six degrees of freedom.

FORMULATION OF PROBLEM

Consider a cylinder, whose cross section is a simply connected region, which is fully or partially immersed horizontally in a previously undisturbed fluid of infinite depth. The body is forced into simple harmonic motion, and it is assumed that steady state conditions have been attained.

The two-dimensional nature of the problem implies three degrees of freedom of motion. Therefore, consider the following three types of oscillatory motions: vertical or heave, horizontal or sway, and rotational about a horizontal axis or roll.

To use linearized free-surface theory, the following assumptions are made:

1. The fluid is incompressible and inviscid.
2. The effects of surface tension are negligible.
3. The fluid flow is irrotational.
4. The motion amplitudes and velocities are all small enough that all but the linear terms of the free surface condition, the kinematic boundary condition on the cylinder, and the Bernoulli equation may be neglected.

For complete discussions of linearized free-surface theory, the reader is referred to Stoker[11] and Wehausen and Laitone.[12]

Given the above conditions and assumptions, the problem reduces to the following boundary-value problem of potential theory. The cylinder is forced into the simple harmonic motion $A^{(m)} \cos(\omega t)$ with prescribed radian frequency ω, where the superscript may take on the values 2, 3, and 4 denoting swaying, heaving, and rolling motions, respectively. It is required to find a velocity potential

$$\Phi^{(m)}(x, y; t) = Re\left(\phi^{(m)}(x, y)\, e^{-i\omega t}\right) \qquad [1]$$

satisfying the following conditions:

1. The Laplace equation

$$\Phi^{(m)}_{xx} + \Phi^{(m)}_{yy} = 0 \qquad [2]$$

in the fluid domain, i.e., for $y < 0$ outside the cylinder;

2. The free surface condition

$$\Phi_{tt}^{(m)} + g\Phi_y^{(m)} = 0 \qquad [3]$$

on the free surface $y = 0$ outside the cylinder, g denoting the acceleration of gravity;

3. The "bottom" condition

$$\lim_{y \to -\infty} |\nabla\Phi^{(m)}| = 0 \qquad [4]$$

4. The condition of the normal velocity component of the fluid at the surface of the cylinder being equal to the normal component of the forced velocity of the cylinder, i.e., if v_n is the component of the forced velocity of the cylinder in the direction of the outgoing unit normal vector n, then

$$n \cdot \nabla\Phi^{(m)} = v_n \qquad [5]$$

this kinematic boundary condition being satisfied at the mean (rest) position of the cylindrical surface; and

5. The radiation condition that the disturbed surface of the fluid takes the form of regular progressive outgoing gravity waves at large distances from the cylinder.

According to Wehausen and Laitone, the complex potential at s of a pulsating point source of unit strength at the point ζ in the lower half plane is

$$G^*(s, \zeta; t) = \frac{1}{2\pi}\left[\log(s - \zeta) - \log(s - \bar{\zeta}) + 2\,P.V.\int_0^\infty \frac{e^{-ik(s-\bar{\zeta})}}{\nu - k}\,dk\right]\cos\omega t - e^{-i\nu(s-\bar{\zeta})}\sin\omega t \qquad [6]$$

so that the real point-source potential is

$$H(x, y, \xi, \eta; t) = Re\,\{G^*(s, \zeta; t)\} \qquad [7]$$

where $z = x + iy$,

$\zeta = \xi + i\eta$, and

$\nu = \omega^2/g$.

Letting

$$G(z, \zeta) = Re\,\frac{1}{2\pi}\left[\log(z-\zeta) - \log(z-\bar{\zeta}) + 2\,P.V.\int_0^\infty \frac{e^{-ik(z-\bar{\zeta})}}{\nu - k}\,dk\right] - i\,Re\left[e^{-i\nu(z-\bar{\zeta})}\right] \qquad [8]$$

then

$$H(x, y, \xi, \eta; t) = Re\left\{G(z, \zeta)\,e^{-i\omega t}\right\} \qquad [9]$$

Equation [9] satisfies the radiation condition and Equations [1] through [4]. Another expression satisfying all these relations is

$$H\left(x, y, \xi, \eta; t - \frac{\pi}{2\omega}\right) = Re\left\{iG(z, \zeta)\,e^{-i\omega t}\right\} \qquad [10]$$

Since the problem is linear, a superposition of Equations [9] and [10] results in the velocity potential

$$\Phi^{(m)}(x, y; t) = Re\int_{C_0} Q(s)\,G(z, \zeta)\,e^{-i\omega t}\,ds \qquad [11]$$

where C_0 is the submerged contour of the cylindrical cross section at its mean (rest) positions and $Q(s)$ represents the complex source density as a function of position along C_0. Application of the kinematic boundary condition on the cylinder at s yields

$$Re\,(n \cdot \nabla)\int_{C_0} Q(s)\,G(z, \zeta)\,ds = 0$$
$$Im\,(n \cdot \nabla)\int_{C_0} Q(s)\,G(z, \zeta)\,ds = A^{(m)}\,\omega\,n^{(m)} \qquad [12]$$

where $A^{(m)}$ denotes the amplitude of oscillation and $n^{(m)}$ the direction cosine of the normal velocity at s on the cylinder. (Both $A^{(m)}$ and $n^{(m)}$ depend on the mode of motion of the cylinder, as will be shown in the following section.) The fact that $Q(s)$ is complex implies that Equations [12] represent a set of two coupled integral equations for the real functions $Re\{Q(s)\}$ and $Im\{Q(s)\}$. The solution of these integral equations and the evaluation of the kernel and potential integrals are described in the following section and in Appendices B and C, respectively.

SOLUTION OF PROBLEM

Take the x axis to be coincident with the undisturbed free surface of a conventional two-dimensional Cartesian coordinate system. Let the cross sectional contour C_0 of the submerged portion of the cylinder be in the lower half plane, the y axis being the axis of symmetry of C_0. (Since ship sections are symmetrical, this investigation is confined to bodies with right and left symmetry.) Select $N+1$ points (ξ_1, η_1), (ξ_2, η_2), $\ldots$, (ξ_N, η_N), and (ξ_{N+1}, η_{N+1}) of C_0 to lie in the fourth quadrant so that (ξ_1, η_1) is located on the negative y axis. For partially immersed cylinders, (ξ_{N+1}, η_{N+1}) is on the positive x axis. For fully submerged bodies, $\xi_{N+1} = \xi_1$, and $\eta_{N+1} < 0$. Connecting these $N+1$ points by successive straight lines, N straight line segments are obtained which, together with their reflected images in the third quadrant, yield an approximation to the given contour as shown in Figure 1. The coordinates, length, and angle associated with the jth segment are identified by the subscript j, whereas the corresponding quantities for the reflected image in the third quadrant are denoted by the subscript $-j$, so that by symmetry $\xi_{-j} = -\xi_j$, and $\eta_{-j} = \eta_j$ for $1 \leq j \leq N+1$.

Potentials and pressures are to be evaluated at the midpoint of each segment. The coordinates of the midpoint of the ith segment are

$$x_i = (\xi_i + \xi_{i+1})/2, \; y_i = (\eta_i + \eta_{i+1})/2 \qquad [13]$$

for $1 \leq i \leq N$. The length of the ith segment is

$$|s_i| = \sqrt{(\xi_{i+1} - \xi_i)^2 + (\eta_{i+1} - \eta_i)^2} \qquad [14]$$

while the angle made by the ith segment with the positive x axis is given by

$$\alpha_i = \tan^{-1} \frac{\eta_{i+1} - \eta_i}{\xi_{i+1} - \xi_i} \qquad [15]$$

The outgoing unit vector normal to the cross section at the ith midpoint (x_i, y_i) is

$$n_i = i \sin \alpha_i - j \cos \alpha_i \qquad [16]$$

where i and j are unit vectors in the directions of increasing x and y, respectively.

The cylinder is forced into simple harmonic motion with radian frequency ω, according to the displacement equation

$$\xi^{(m)} = A^{(m)} \cos \omega t \qquad [17]$$

for $m = 2$, 3, or 4, corresponding to sway, heave, or roll, respectively. The rolling oscillations are about an axis through a point $(0, y_0)$ in the symmetry plane of the cylinder.

In the translational modes, any point of the cylinder moves with velocity

$$v^{(2)} = -i A^{(2)} \omega \sin \omega t \qquad [18]$$

for sway, or

$$v^{(3)} = -j A^{(3)} \omega \sin \omega t \qquad [19]$$

for heaving oscillations.

Rolling motion about $(0, y_0)$ is illustrated in Figure 2. Considering a point (x_i, y_i) on C_0, an inspection of Figure 2 yields

$$R_i = \sqrt{x_i^2 + (y_i - y_0)^2}$$

and

$$\theta_i = \tan^{-1} \frac{y_1 - y_0}{x_i} = \sin^{-1} \frac{y_i - y_0}{R_i} = \cos^{-1} \frac{x_i}{R_i}$$

Therefore, by elementary two-dimensional kinematics, the unit vector in the direction of increasing θ is

$$\tau_i = -i \sin \theta_i + j \cos \theta_i = -\frac{y_i - y_0}{R_i} i + \frac{x_i}{R_i} j$$

so that

$$v^{(4)} = R_i \, S^{(4)} \, \tau_i = \omega \, A^{(4)} \, [(y_i - y_0) \, i - x_i \, j] \sin \omega t \qquad [20]$$

The normal components of the velocity $v_i^{(m)} = n_i \cdot v^{(m)}$ at the midpoint of the ith segment (x_i, y_i) are

$$\begin{aligned} v_i^{(2)} &= -\omega \, A^{(2)} \sin \alpha_i \sin \omega t \\ v_i^{(3)} &= \omega \, A^{(3)} \cos \alpha_i \sin \omega t \\ v_i^{(4)} &= \omega \, A^{(4)} \, [(y_i - y_0) \sin \alpha_i + x_i \cos \alpha_i] \sin \omega t \end{aligned} \qquad [21]$$

for the swaying, heaving, and rolling modes, respectively. Defining

$$n_i^{(m)} = \frac{v_i^{(m)}}{A^{(m)} \, \omega \sin \omega t}$$

then, consistent with the previously mentioned notation, the direction cosines for the three modes of motion are

$$\begin{aligned} n_i^{(2)} &= -\sin \alpha_i \\ n_i^{(3)} &= \cos \alpha_i \\ n_i^{(4)} &= (y_i - y_0) \sin \alpha_i + x_i \cos \alpha_i \end{aligned} \qquad [22]$$

Equations [22] illustrate that heaving is symmetrical, i.e., $n_{-i}^{(3)} = n_i^{(3)}$. Swaying and rolling, however, are antisymmetrical modes, i.e., $n_{-i}^{(2)} = -n_i^{(2)}$, and $n_{-i}^{(4)} = -n_i^{(4)}$.

Equations [12] are applied at the midpoints of each of the N segments, and it is assumed that over an individual segment the complex source strength $Q(s)$ remains constant, although it varies from segment to segment. With these stipulations, the set of coupled integral Equations [12] becomes a set of $2N$ linear algebraic equations in the unknowns

$$Re \, [Q^{(m)}(s_j)] = Q_j^{(m)} \quad \text{and} \quad Im \, [Q^{(m)}(s_j)] = Q_{N+j}^{(m)}$$

Thus, for $i = 1, 2, \ldots, N$

$$\sum_{j=1}^{N} Q_j^{(m)} I_{ij}^{(m)} + \sum_{j=1}^{N} Q_{N+j}^{(m)} J_{ij}^{(m)} = 0$$

$$- \sum_{j=1}^{N} Q_j^{(m)} J_{ij}^{(m)} + \sum_{j=1}^{N} Q_{N+j}^{(m)} I_{ij}^{(m)} = \omega A^{(m)} n_i^{(m)} \qquad [23]$$

where the superscript (m) denotes the mode of motion. The "influence coefficients" $I_{ij}^{(m)}$ and $J_{ij}^{(m)}$ and the potential $\Phi^{(m)}(x_i, y_i; t)$ are evaluated in the appendix. The resulting velocity potential consists of a term in phase with the displacement* and a term in phase with the velocity.

The hydrodynamic pressure at (x_i, y_i) along the cylinder is obtained from the velocity potential by means of the linearized Bernoulli equation

$$p^{(m)}(x_i, y_i, \omega; t) = -\rho \Phi_t^{(m)}(x_i, y_i, \omega; t) \qquad [24]$$

as

$$p^{(m)}(x_i, y_i, \omega; t) = p_a^{(m)}(x_i, y_i; \omega) \cos \omega t + p_v^{(m)}(x_i, y_i; \omega) \sin \omega t \qquad [25]$$

where $p_a^{(m)}$ and $p_v^{(m)}$ are the hydrodynamic pressures in phase with the displacement and in phase with the velocity, respectively. (ρ denotes the density of the fluid in Equation [24]). As indicated by the notation of Equations [24] and [25], the pressure as well as the potential is a function of the oscillation frequency.

The hydrodynamic force or moment (when $m = 4$) per unit length along the cylinder necessary to sustain the oscillations is the integral of $p^{(m)} \cdot n^{(m)}$ over the submerged contour of the cross section C_0. It is assumed that the pressure at the ith midpoint is the mean pressure for the ith segment, so that integration reduces to summation, whence

$$M^{(m)}(\omega) = 2 \sum_{j=1}^{N} p_a^{(m)}(x_i, y_i; \omega) n_i^{(m)} \qquad [26]$$

and

$$N^{(m)}(\omega) = 2 \sum_{j=1}^{N} p_v^{(m)}(x_i, y_i; \omega) n_i^{(m)} \qquad [27]$$

for the added mass and the damping forces or moments, respectively.

*Most authors refer to this term as a component in phase with the acceleration. However, due to displacement Equation [17], this author deems it more appropriate to refer to this term as being 180 degrees out-of-phase with the acceleration or in-phase with the displacement.

The velocity potentials for very small and very large frequencies are derived and discussed in Appendix D.

LIMITATIONS OF GREEN'S FUNCTION – INTEGRAL EQUATION METHOD

F. John[13] proved the existence and uniqueness of the solutions to the three- and two-dimensional potential problems pertaining to oscillations of rigid bodies in a free surface. The solutions were subject to the provisions that no point of the immersed surface of the body would be outside a cylinder drawn vertically downward from the intersection of the body with the free surface and that the free surface would be intersected orthogonally by the body in its mean or rest position.

John also showed that for a set of discrete "irregular" frequencies the Green's function-integral equation method failed to give a solution. He demonstrated that the irregular frequencies occurred when the following adjoint interior-potential problem had eigenfrequencies. Let $\psi(x, y)$ be such that

1. $\psi_{xx} + \psi_{yy} = 0$ inside the cylinder in the region bounded by the immersed surface of the body and the extension of the free surface inside the cylinder;

2. $\psi_y - \nu_k \psi = 0$ on the extension of the free surface inside the cylinder, ν_k being the wave number corresponding to the irregular frequency ω_k, $k = 1, 2, 3, \ldots$;

3. $\psi = 0$ on the surface of the cylinder below the free surface.

For a rectangular cylinder with beam B and draft T (see Figure 3), the irregular wave numbers may be easily obtained by separation of variables in the Laplace equation. Separating variables gives the eigenfunctions

$$\psi_k = B_k \sin (k \pi x/B) \sinh (k \pi T/B)$$

for $k = 1, 2, 3, \ldots$, etc., where the B_k are Fourier coefficients to be determined from an appropriate boundary condition. Applying the free-surface condition (2) on $y = T$ for $0 < x < B$, the eigenwave numbers (or irregular wave numbers)

$$\nu_k = (k \pi/B) \coth (k \pi T/B) \qquad [28]$$

are obtained for $k = 1, 2, \ldots$, etc. In particular, the lowest such irregular wave number is given by

$$\nu_1 = (\pi/B) \coth (\pi T/B) \qquad [29]$$

Keeping T fixed in Equation [29] but letting B vary and setting $\delta = \pi/B$, then from the Taylor expansion

$$\delta \coth (\delta T) = \delta \left[1/(\delta T) + \delta T/3 - (\delta T)^3/45 + \ldots\right]$$

it is seen that as $\delta \to 0$, which is equivalent to $B \to \infty$, $\nu_1 \to 1/T$. Therefore, for rectangular cylinders of draft T,

$$\nu_1 \geq 1/T \qquad [30]$$

a relation that John proved for general shapes complying with the restrictions previously outlined. Figure 4 depicts the first irregular wave number for rectangular cylinders as a function of the beam-to-draft ratio, keeping the draft constant. For a beam-to-draft ratio of 2.5, $\nu_1 \doteq 1.48$; while for $B/T = 2$, $\nu_1 \doteq 1.71$.

At an irregular frequency the matrix of influence coefficients of Equations [28] becomes singular as the number of defining points per cross section increases without limit, i.e., as $N \to \infty$. In practice, with finite N, the determinant of this matrix becomes very small not only at the irregular frequency but also in an interval about this frequency. This interval can be reduced by increasing the number of defining points N for the cross section. Figures 5, 6, and 7 illustrate this phenomenon and its effect on the calculated added mass and damping coefficients.

These results are significant in the application to ship sections. Most surface vessels have nearly constant draft over the length of the ship, and the maximum beam occurs at or near midship, where the cross section is usually almost rectangular, so that for most surface ships the first irregular frequency ω_1 is less for the midsection than for any other cross section. For a ship with a 7:1 length-to-beam and a 5:2 beam-to-draft, the first irregular wave encounter frequency--in nondimensional form with L denoting the ship length--occurs at

$$\omega_1 \sqrt{L/g} \approx 5.09$$

which is beyond the range of practical interest for ship-motion analysis. Therefore, for slender surface vessels, the phenomenon of the first irregular frequency of wave encounter is not too important.

NUMERICAL RESULTS AND CONCLUSIONS

A computer program, based on the analysis of this report, was developed, and calculations for cylinders of various cross sections were performed by the IBM 7090 electronic digital computer at the Center. Two options in the program provide for pressure and added mass or moment calculations for the asymptotic cases of very small and very large frequencies.

The most time consuming computer operations occur when evaluating the principal value integrals. These integrals are of the complex exponential integral type and are calculated as power series in νr, with $r^2 = (x_i - \xi_j)^2 + (y_i + \eta_j)^2$, and $\nu = \omega^2/g$. These series (derived in the appendix) converge fairly rapidly for partially submerged shiplike sections at frequencies lower than the first irregular frequency. This results in an average computer time of 20 seconds per frequency for half sections defined by 21 input points. However, for fully immersed bodies, r is considerably larger, so that the much slower convergence of the series increases the computation time greatly. For a given contour and frequency the computer time varies as the square of the number of input points, which is limited to a mesh fineness of 46 points per half section.

The frequency input to this program is in the form of wave numbers, nondimensionalized by some principal linear dimension such as the draft or the half beam. The output of this computer program includes the pressures in phase with the displacement and in phase with the velocity at each of the segmental midpoints, the added mass or added moment and damping coefficients in normalized form, and a scaled version of the determinant of the matrix of influence coefficients.

For partially submerged cylinders the added mass or moment and the damping are scaled by ω^2 times the amplitude of oscillation times the displaced mass or displaced moment of inertia of a semicircular cylinder of radius equal to the principal dimension. For fully immersed bodies these quantities are normalized by ω^2 times the oscillation amplitude times the displaced mass or displaced moment of inertia of a circular cylinder of radius equal to the principal dimension. It is assumed in all cases that the cylinders are oscillating with unit amplitude

The graphs of Figures 5 through 26 were obtained with the aid of the SC 4020 Charactron plotter, an important piece of peripheral equipment to the IBM 7090 digital computer. These figures illustrate the behavior of the hydrodynamic pressure and normalized force components as functions of the nondimensional wave number for various cylindrical shapes. In Figures 8 through 13, the added mass and damping coefficients as well as the hydrodynamic pressure components are plotted against $\omega^2 B/(2g)$ for the heaving and swaying semi-immersed circular cylinder, defined by 21 equally spaced input points around the half section. The results for the heaving mode agree well with the Porter results. Figure 14 depicts the added mass and damping coefficients of a fully submerged heaving circular cylinder, defined by 21 equally spaced points, whose axis is submerged to a depth of 1.25 times

its radius. The values obtained in this case are in good agreement with the results obtained by Ogilvie from his first order theory. Figures 15 through 17 show the added mass, damping, and pressures of a partially immersed heaving ogival cylinder with draft/diameter equal to 9/10 and beam/diameter equal to 3/5 as functions of the nondimensional wave number $\omega^2 B/(2g)$. This is an instance of a bulbuous section similar to the cylinders discussed by Motora and Koyama,[14] which have the property that the damping vanishes at some frequency. Figure 15 indicates zero damping at about $\omega^2 B/(2g) = 0.7$.

Figures 18 through 20 illustrate the added mass, added moment, and damping coefficients for all three modes of oscillation of a cylinder whose cross section is in the shape of the midsection of a Series 60, Block 70 ship defined by 16 input points per half section as well as the same parameters for a geometry defined by only 7 input points. The close agreement between these two sets of output data (within 10 percent of each other) suggest the possibility of using a coarse sectional input mesh for the application of this method to the strip theory of ship motions. The computing time for the 16 point geometry was roughly six times that for the 7 point half section. The graphs in Figure 18 are very similar to the curves for the added mass and damping coefficients of the heaving, full-form, Lewis-type cylinder of Porter. Figures 21 through 26 show the sway, heave, roll, added mass or moment and damping coefficients for the bow and stern sections of the same ship, defined by 7 points per half section. Observe that the roll damping for these sections is considerably larger than for the midsection, being largest for the extremely slim bow section.

Recall that three assumptions were made to obtain numerical solutions to the boundary-value problem. First, it was assumed that the cylindrical cross section could be approximated by a polygonal succession of straight-line segments defined by a finite number of points. Second, the hypothesis of the constancy of the source strengths along an individual segment was employed to convert the integral equations into a set of linear algebraic equations. Third, the supposition of mean hydrodynamic pressures over the individual segments made it possible for the integrations of these pressures to be transformed into summations. However, as the number of segments is made to increase indefinitely, while the largest of these segments converges to zero length, the polygonal approximation approaches the cross sectional contour, and the source strengths and pressures become continuous functions of position (and frequency) along this contour.

The Green's function-integral equation method as described in this paper is applicable to any two-dimensional simply connected shape (even those with severe corners, bilge keels, bulbs, fins, etc.), whereas the mapping of these odd-shaped contours onto the unit circle requires a great number of terms in the Theodorsen transformation. Smith reported the necessity of obtaining 16 Theodorsen coefficients for the mapping of a bulbous form with an expenditure of 8 minutes of computer time.

ACKNOWLEDGMENTS

The author acknowledges the many valuable criticisms and suggestions offered by Drs. T. F. Ogilvie, J. N. Newman, C. M. Lee, and E. O. Tuck, who pointed out the phenomenon of the irregular frequencies to the author. Mrs. S. E. Good and Mr. L. F. Mueller furnished many valuable hints for the construction of the computer program.

APPENDIX A

EVALUATION OF PRINCIPAL VALUE INTEGRAL

The real and imaginary parts of the principal value integral

$$P.V.\int_0^\infty \frac{e^{-ik(z\ \bar{\zeta})}}{\nu - k}\, dk$$

are used in evaluating some of the kernel and potential integrals.

The residue of the integrand at $k = \nu$ is $e^{-i\nu(z-\zeta)}$, so that

$$P.V.\int_0^\infty \frac{e^{-ik(z-\bar{\zeta})}}{\nu-k}\, dk = \int_0^\infty \frac{e^{-ik(z-\bar{\zeta})}}{\nu-k}\, dk + i\pi e^{-i\nu(z-\bar{\zeta})} \qquad [31]$$

where the path of integration is the positive real axis indented into the upper half plane about $k = \nu$.

Note that $\nu = \omega^2/g > 0$, $Im\ z < 0$, and $Im\ \zeta \leq 0$. The transformation $w = i(k-\nu)(z-\bar{\zeta})$ converts the contour integral on the right side of Equation [31] to

$$\begin{aligned}\int_0^\infty \frac{e^{-ik(z-\bar{\zeta})}}{\nu-k}\, dk &= -e^{-i\nu(z-\bar{\zeta})}\int_{-i\nu(z-\bar{\zeta})}^\infty \frac{e^{-w}}{w}\, dw \\ &= -e^{-i\nu(z-\bar{\zeta})}\, E_1\,[-i\nu(z-\bar{\zeta})] \\ &= e^{-i\nu(z-\zeta)}\left\{\gamma + \log\,[-i\nu(z-\bar{\zeta})]\right. \\ &\quad \left. + \sum_{n=1}^{\infty} \frac{(-1)^n[-i\nu(z-\bar{\zeta})]^n}{n\,n!}\right\}\end{aligned} \qquad [32]$$

where $\gamma = 0.5772\ldots$ is the well known Euler-Mascheroni constant. (See Abramovitz and Stegun[15] for the definition of E_1.)

Setting $r = |-i\nu(z-\bar{\zeta})|$ and

$$\theta = \tan^{-1}\,[Im\,(-i\nu(z-\bar{\zeta}))/Re\,(-i\nu(z-\bar{\zeta}))] + \pi$$

the following expression is obtained for Equation [31]

$$P.V. \int_0^\infty \frac{e^{-ik(x-\zeta)}}{\nu - k}\, dk = e^{\nu(y+\eta)}\left[\cos \nu(x-\xi) - i \sin \nu(x-\xi)\right]$$

$$\cdot\left\{\left[\gamma + \log r + \sum_{n=1}^{\infty} \frac{r^n \cos(n\theta)}{n \cdot n!}\right]\right. \qquad [33]$$

$$\left. + i\left[\theta + \sum_{n=1}^{\infty} \frac{r^n \sin(n\theta)}{n \cdot n!}\right]\right\}$$

Separating Equation [33] into its real and imaginary parts yields

$$P.V. \int_0^\infty \frac{e^{(y+\eta)k} \cos k(x-\xi)}{\nu - k}\, dk = e^{\nu(y+\eta)}\left[C(r,\theta) \cos \nu(x-\xi)\right.$$

$$\left. + S(r,\theta) \sin \nu(x-\xi)\right] \qquad [34]$$

$$P.V. \int_0^\infty \frac{e^{(y+\eta)k} \sin k(x-\xi)}{\nu - k}\, dk = e^{\nu(y+\eta)}\left[C(r,\theta) \sin \nu(x-\xi)\right.$$

$$\left. - S(r,\theta) \cos \nu(x-\xi)\right]$$

provided that

$$C(r,\theta) = \gamma + \log r + \sum_{n=1}^{\infty} \frac{r^n \cos(n\theta)}{n \cdot n!}$$

and

$$S(r,\theta) = \theta + \sum_{n=1}^{\infty} \frac{r^n \sin(n\theta)}{n \cdot n!}$$

APPENDIX B

EVALUATION OF KERNEL INTEGRALS

The influence coefficients of Equations [23] are

$$I_{ij}^{(m)} = Re \left\{ (n_i \cdot \nabla) \left[\int_{s_j} \left[\frac{1}{2\pi} \left(\log (z - \bar{\zeta}) - \log (z - \bar{\zeta}) \right) + \frac{1}{\pi} P.V. \int_0^\infty \frac{e^{-ik(z - \bar{\zeta})}}{\nu - k} dk \right] ds \right. \right.$$

$$\left. \left. - (-1)^m \int_{s_{-j}} \left[\frac{1}{2\pi} \left(\log (z + \bar{\zeta}) - \log (z + \zeta) \right) + \frac{1}{\pi} P.V. \int_0^\infty \frac{e^{-ik(z + \zeta)}}{\nu - k} dk \right] ds \right] \right|_{z = z_i} \right\} \quad [35]$$

and

$$J_{ij}^{(m)} = Re \left\{ (n_i \cdot \nabla) \left[\int_{s_j} e^{-i\nu(z - \bar{\zeta})} ds - (-1)^m \int_{s_{-j}} e^{-i\nu(z + \zeta)} ds \right] \right|_{z = z_i} \right\} \quad [36]$$

We note that in the complex plane with s_i on s_i,

$$Re \left\{ (n_i \cdot \nabla) F(z) \Big|_{z = z_i} \right\} = Re \left\{ -ie^{i\alpha_i} \frac{dF(z)}{dz} \Big|_{z = z_i} \right\}$$

Considering the term containing $\log (z - \zeta)$, it is evident that the kernel integral is singular when $i = j$, so that the indicated differentiation cannot be performed under the integral sign. However, in that case one may proceed as follows:

since

$$\zeta = \xi + i\eta$$

$$d\zeta = d\xi + id\eta$$

$$= ds \cos \alpha_j + ids \sin \alpha_j$$

$$= e^{i\alpha_j} ds$$

for ζ along the jth segment. Therefore, $ds = e^{-i\alpha_j} d\zeta$, and

$$Re \left\{ (n_j \cdot \varphi) \int_{s_j} \log (z - \zeta)\, ds \,\Big|_{z=z_j} \right\}$$

$$= Re \left\{ -ie^{i\alpha_j} \frac{d}{dz} \int_{\zeta_j}^{\zeta_{j+1}} e^{-i\alpha_j} d\zeta \log (z - \zeta) \,\Big|_{z=z_j} \right\}$$

$$= Re \left\{ -i \frac{d}{dz} \int_{\zeta_j}^{\zeta_{j+1}} \log (z - \zeta)\, d\zeta \,\Big|_{z=z_j} \right\}$$

Setting $\zeta' = z - \zeta$, the last integral becomes

$$Re \left\{ -i \frac{d}{dz} \int_{z-\zeta_{j+1}}^{z-\zeta_j} \log \zeta'\, d\zeta' \,\Big|_{z=z_j} \right\} \qquad [37]$$

$$= \arg (z_j - \zeta_j) - \arg (z_j - \zeta_{j+1}) = \pi$$

If $i \neq j$, differentiation under the integral sign may be performed, so that

$$Re \left\{ (n_i \cdot \varphi) \int_{s_j} \log (z - \zeta)\, ds \,\Big|_{z=z_i} \right\}$$

$$= \sin (\alpha_i - \alpha_j) \log \sqrt{\frac{(x_i - \xi_j)^2 + (y_i - \eta_j)^2}{(x_i - \xi_{j+1})^2 + (y_i - \eta_{j+1})^2}} \qquad [38]$$

$$+ \cos (\alpha_i - \alpha_j) \left[\tan^{-1} \frac{y_i - \eta_j}{x_i - \xi_j} - \tan^{-1} \frac{y_i - \eta_{j+1}}{x_i - \xi_{j+1}} \right]$$

For the integral containing the log $(z - \bar{\zeta})$ term, $ds = e^{i\alpha_j}\, d\bar{\zeta}$, so that

$$Re\left\{(n_i \cdot \nabla) \int_{s_j} \log (z - \bar{\zeta})\, ds \,\Big|_{z = z_i}\right\}$$

$$= \sin (\alpha_i + \alpha_j) \log \sqrt{\frac{(x_i - \xi_j)^2 + (y_i + \eta_j)^2}{(x_i - \xi_{j+1})^2 + (y_i + \eta_{j+1})^2}} \qquad [39]$$

$$+ \cos (\alpha_i + \alpha_j) \left[\tan^{-1} \frac{y_i + \eta_j}{x_i - \xi_j} - \tan^{-1} \frac{y_i + \eta_{j+1}}{x_i - \xi_{j+1}}\right]$$

The kernel integral containing the principal value integrals is

$$Re\left\{(n_i \cdot \nabla) \int_{s_j} ds\, P.V. \int_0^\infty \frac{e^{-ik(z - \bar{\zeta})}}{\nu - k}\, dk \,\Big|_{z = z_i}\right\}$$

$$= Re\left\{-ie^{i(\alpha_i + \alpha_j)} \int_{\bar{\zeta}_{j+1}}^{\bar{\zeta}_j} d\bar{\zeta}\, \frac{d}{d\bar{\zeta}}\, P.V. \int_0^\infty \frac{e^{-ik(z_i - \bar{\zeta})}}{\nu - k}\, dk\right\}$$

$$= \sin (\alpha_i + \alpha_j) \left[P.V. \int_0^\infty \frac{e^{k(y_i + \eta_j)} \cos k(x_i - \xi_j)}{\nu - k}\, dk\right. \qquad [40]$$

$$\left. - P.V. \int_0^\infty \frac{e^{k(y_i + \eta_{j+1})} \cos k (x_i - \xi_{j+1})}{\nu - k}\, dk\right]$$

$$- \cos (\alpha_i + \alpha_j) \left[P.V. \int_0^\infty \frac{e^{k(y_i + \eta_j)} \sin k(x_i - \xi_j)}{\nu - k}\, dk\right.$$

$$\left. - P.V. \int_0^\infty \frac{e^{k(y_i + \eta_{j+1})} \sin k(x_i - \xi_{j+1})}{\nu - k}\, dk\right]$$

The first integral on the right side of Equation [36] becomes

$$Re\left\{(n_i \cdot \nabla) \int_{s_j} e^{-i\nu(z - \bar{\zeta})}\, ds \,\Big|_{z = z_i}\right\}$$

$$= -\sin (\alpha_i + \alpha_j) \left[e^{\nu(y_i + \eta_j)} \cos \nu(x_i - \xi_j) - e^{\nu(y_i + \eta_{j+1})} \cos \nu(x_i - \xi_{j+1})\right] \qquad [41]$$

$$+ \cos (\alpha_i + \alpha_j) \left[e^{\nu(y_i + \eta_j)} \sin \nu(x_i - \xi_j) - e^{\nu(y_i + \eta_{j+1})} \sin \nu(x_i - \xi_{j+1})\right]$$

The kernel integrals over the image segments are obtained from Equations [38] through [41] by replacing ξ_j, ξ_{j+1}, and α_j with $\xi_{-j} = -\xi_j$, $\xi_{-(j+1)} = -\xi_{j+1}$, and $\alpha_{-j} = -\alpha_j$, respectively.

APPENDIX C

EVALUATION OF POTENTIAL INTEGRALS

The velocity potential for the mth mode of oscillation at the ith midpoint (x_i, y_i) is

$$\begin{aligned}\Phi^{(m)}(x_i, y_i; t) = \frac{1}{2\pi} \sum_{j=1}^{N} Q_j \, Re \left\{ \int_{s_j} \left[\log (z_i - \zeta) - \log (z_i - \bar{\zeta}) \right.\right. \\ \left. + 2 \, P.V. \int_0^\infty \frac{e^{-ik(z_i - \bar{\zeta})}}{\nu - k} \, dk \right] ds \\ - (-1)^m \int_{s_{-j}} \left[\log (z_i + \bar{\zeta}) - \log (z_i + \zeta) \right. \\ \left.\left. + 2 \, P.V. \int_0^\infty \frac{e^{-ik(z_i + \zeta)}}{\nu - k} \, dk \right] ds \right\} \cdot \cos \omega t \\ - \sum_{j=1}^{N} Q_{N+j} \, Re \left\{ \int_{s_j} e^{-i\nu(z_i - \bar{\zeta})} \, ds \right. \\ \left. - (-1)^m \int_{s_{-j}} e^{-i\nu(z_i + \zeta)} \, ds \right\} \cdot \sin \omega t\end{aligned} \qquad [42]$$

The integration of the $\log (z_i - \zeta)$ term is straightforward, yielding

$$\begin{aligned}Re \left\{ \int_{s_j} \log (z_i - \zeta) \, ds \right\} \\ = \cos \alpha_j \left[(x_i - \xi_j) \log \sqrt{(x_i - \xi_j)^2 + (y_i - \eta_j)^2} + \xi_j - \xi_{j+1} \right. \\ - (x_i - \xi_{j+1}) \log \sqrt{(x_i - \xi_{j+1})^2 + (y_i - \eta_{j+1})^2} \\ \left. - (y_i - \eta_j) \tan^{-1} \frac{(y_i - \eta_j)}{(x_i - \xi_j)} + (y_i - \eta_{j+1}) \tan^{-1} \frac{(y_i - \eta_{j+1})}{(x_i - \xi_{j+1})} \right]\end{aligned} \qquad [43]$$

$$+ \sin \alpha_j \left[(y_i - \eta_j) \log \sqrt{(x_i - \xi_j)^2 + (y_i - \eta_j)^2} + \eta_j - \eta_{j+1} \right.$$
$$- (y_i - \eta_{j+1}) \log \sqrt{(x_i - \xi_{j+1})^2 + (y_i - \eta_{j+1})^2} \qquad [43]$$
$$\left. + (x_i - \xi_j) \tan^{-1} \frac{(y_i - \eta_j)}{(x_i - \xi_j)} - (x_i - \xi_{j+1}) \tan^{-1} \frac{(y_i - \eta_{j+1})}{(x_i - \xi_{j+1})} \right]$$

In the integration of the $\log (z - \bar{\zeta})$ term, note that η_j and η_{j+1} are replaced by $-\eta_j$ and $-\eta_{j+1}$, respectively.

To evaluate the potential integral containing the principal value integral, proceed in the following manner. For an arbitrary s in the fluid domain

$$\int_{\bar{\zeta}_j}^{\bar{\zeta}_{j+1}} ds \; P.V. \int_0^\infty \frac{e^{-ik(z-\zeta)}}{\nu - k} \, dk$$

$$= e^{i\alpha_j} P.V. \int_0^\infty \frac{dk}{\nu - k} \int_{\bar{\zeta}_j}^{\bar{\zeta}_{j+1}} e^{-ik(z-\bar{\zeta})} \, d\bar{\zeta}$$

$$= e^{i\alpha_j} P.V. \int_0^\infty \frac{e^{-ikz}}{\nu - k} \, dk \int_{\bar{\zeta}_j}^{\bar{\zeta}_{j+1}} e^{ik\bar{\zeta}} \, d\bar{\zeta}$$

$$= -ie^{i\alpha_j} P.V. \int_0^\infty \frac{e^{-ikz}}{\nu - k} \frac{(e^{ik\bar{\zeta}_{j+1}} - e^{ik\bar{\zeta}_j})}{k} \, dk$$

where the change of integration is permissible since only one integral requires a principal value interpretation. After dividing by ν and multiplying by $\nu - k + k$ under the integral sign, the last expression becomes

$$- \frac{ie^{i\alpha_j}}{\nu} \left[\int_0^\infty e^{-ikz} \frac{(e^{ik\bar{\zeta}_{j+1}} - e^{ik\bar{\zeta}_j})}{k} \, dk \right.$$
$$\left. + P.V. \int_0^\infty \frac{e^{-ik(z-\bar{\zeta}_{j+1})}}{\nu - k} \, dk - P.V. \int_0^\infty \frac{e^{-ik(z-\bar{\zeta}_j)}}{\nu - k} \, dk \right] \qquad [44]$$

Regarding the first integral in Equation [44] as a function of z,

$$F(z) = \int_0^\infty \frac{e^{-ikz}\,(e^{ik\bar{\zeta}_{j+1}} - e^{ik\bar{\zeta}_j})}{k}\,dk \qquad [45]$$

Differentiating Equation [45] with respect to z gives

$$F'(z) = -i\left\{\int_0^\infty e^{-ik\,(z\,-\,\bar{\zeta}_{j+1})}\,dk - \int_0^\infty e^{-ik\,(z\,-\,\bar{\zeta}_j)}\,dk\right\}$$

$$= \frac{1}{z-\bar{\zeta}_j} - \frac{1}{z-\bar{\zeta}_{j+1}}$$

so

$$F(z) = \log(z-\bar{\zeta}_j) - \log(z-\bar{\zeta}_{j+1}) + K \qquad [46]$$

where K is a constant of integration to be determined presently. Since $F(z)$ is defined and analytic for all z in the lower half plane, and since by Equation [45], $\lim_{z\to-\infty i} F(z) = 0$, it follows from Equation [46] that $K = 0$. Therefore,

$$Re\left\{\int_{z_j} dz\ P.V.\int_0^\infty \frac{e^{-ik\,(z_i\,-\,\bar{\zeta})}}{\nu-k}\,dk\right\}$$

$$= Re\left\{-\frac{ie^{i\alpha_j}}{\nu}\left[\log(z_i-\bar{\zeta}_j) - \log(z_i-\bar{\zeta}_{j+1})\right.\right.$$

$$\left.\left. + P.V.\int_0^\infty \frac{e^{-ik\,(z_i\,-\,\bar{\zeta}_{j+1})}}{\nu-k}\,dk - P.V.\int_0^\infty \frac{e^{-ik\,(z_i\,-\,\bar{\zeta}_j)}}{\nu-k}\,dk\right]\right\} \qquad [47]$$

$$= \frac{1}{\nu}\left\{\sin\alpha_j\left[\log\sqrt{\frac{(x_i-\xi_j)^2+(y_i+\eta_j)^2}{(x_i-\xi_{j+1})^2+(y_i+\eta_{j+1})^2}}\right.\right.$$

$$\left.\left. + P.V.\int_0^\infty \frac{e^{k\,(y_i\,+\,\eta_{j+1})}\cos k\,(x_i-\xi_{j+1})}{\nu-k}\,dk\right.\right.$$

$$
\left. - P.V. \int_0^\infty \frac{e^{k(y_i + \eta_j)} \cos k(x_i - \xi_j)}{\nu - k} \, dk \right]
$$

$$
+ \cos \alpha_j \left[\tan^{-1} \frac{(y_i + \eta_j)}{(x_i - \xi_j)} - \tan^{-1} \frac{(y_i + \eta_{j+1})}{(x_i - \xi_{j+1})} \right. \qquad [47]
$$

$$
+ P.V. \int_0^\infty \frac{e^{k(y_i + \eta_j)} \sin k(x_i - \xi_j)}{\nu - k} \, dk
$$

$$
\left. \left. - P.V. \int_0^\infty \frac{e^{k(y_i + \eta_{j+1})} \sin k(x_i - \xi_{j+1})}{\nu - k} \, dk \right] \right\}
$$

The integration of the potential compontent in phase with the velocity over s_j gives

$$
Re \left\{ \int_{s_j} e^{-i\nu(z_i - \bar{\zeta})} \, ds \right\} \qquad [48]
$$

$$
= \frac{1}{\nu} \left\{ e^{\nu(y_i + \eta_j)} \sin \left[\nu(x_i - \xi_j) - \alpha_j \right] - e^{\nu(y_i + \eta_{j+1})} \sin \left[\nu(x_i - \xi_{j+1}) - \alpha_j \right] \right\}
$$

APPENDIX D

VELOCITY POTENTIALS FOR VERY SMALL AND VERY LARGE FREQUENCIES

For very small frequencies, i.e., as $\omega \to 0$, the free-surface condition Equation [3] of the section formulating the problem degenerates into the wall-boundary condition

$$\Phi_y = 0 \qquad [49]$$

on the surface of the fluid outside the cylinder, whereas for extremely large frequencies, i.e., when $\omega \to \infty$, the free-surface condition becomes the "impulsive" surface condition

$$\Phi = 0 \qquad [50]$$

on $y = 0$ outside the cylinder.

Equations [2], [4], and [5] remain valid for both asymptotic cases. The radiation condition is replaced by a condition of boundedness at infinity.

Therefore, there is a Neumann problem for the case $\omega \to 0$ and a mixed problem when $\omega \to \infty$. The appropriate complex potentials for a source of unit strength at a point ζ in the lower half plane are

$$G_0(s, \zeta) = \frac{1}{2\pi}\left[\log(s - \zeta) + \log(s - \bar{\zeta})\right] + K_0 \qquad [51]$$

and

$$G_\infty(s, \zeta) = \frac{1}{2\pi}\left[\log(s - \zeta) - \log(s - \bar{\zeta})\right] + K_\infty \qquad [52]$$

for the Neumann and mixed problems, respectively, where K_0 and K_∞ are constants not yet specified.

Let

$$\phi_a(x, y; \xi, \eta) = Re\left\{G_a(s, \zeta)\right\}$$

so that the velocity potentials for the mth mode of motion are

$$\Phi_a^{(m)}(x, y) = \int_{C_0} Q_a^{(m)}(s)\, \phi_a(x, y; \xi, \eta)\, ds \qquad [53]$$

for $a = 0$, and $a = \infty$, where $Q_a^{(m)}$ is the expression for the source strength as a function of position along the submerged contour of the cross section C_0. An analysis similar to the one in the section on formulating the problem leads to the integral equation

$$(n \cdot \nabla) \int_{C_0} Q_a^{(m)}(s)\, \phi_a(x, y; \xi, \eta)\, ds = A^{(m)}\, n^{(m)} \qquad [54]$$

which, after application at the N segmental midpoint, yields a set of N linear algebraic equations in the N unknown source strengths Q_j.

It remains to be shown whether these two problems are, in the language of potential theory, well posed, i.e., whether the solutions to these problems lead to unique forces or moments. The mixed problem raises no difficulty, since as $s \to \infty$, $G_\infty(s, \zeta) \to 0$. In fact $K_\infty = 0$, which can be inferred from the pulsating source-potential Equation [8] by letting $\nu \to \infty$.

Considering the Neumann problem, note that the constant K_0 in the Green's function Equation [51] yields by integration an additive constant K to the potential. However, for a completely submerged cylinder the cross sectional contour C_0 is a simply closed curve, so that the contribution of K in integrating the product of the pressure with the direction cosine of the body-surface velocity vanishes. For partially submerged bodies C_0 is no longer closed. But since $n_{-i}^{(m)} = -n_i^{(m)}$ for m being even,

$$\int_{C_0} K\, n^{(m)}\, ds = 0$$

so that the swaying force and rolling moment are unique. The heaving force on a partially submerged cylinder is not unique for, in this case, $n_{-i}^{(3)} = n_i^{(3)}$, so that

$$\int_{C_0} K\, n^{(3)}\, ds \neq 0$$

The constant K_0 may be obtained by letting $\nu \to 0$ in the pulsating source-potential Equation [8].

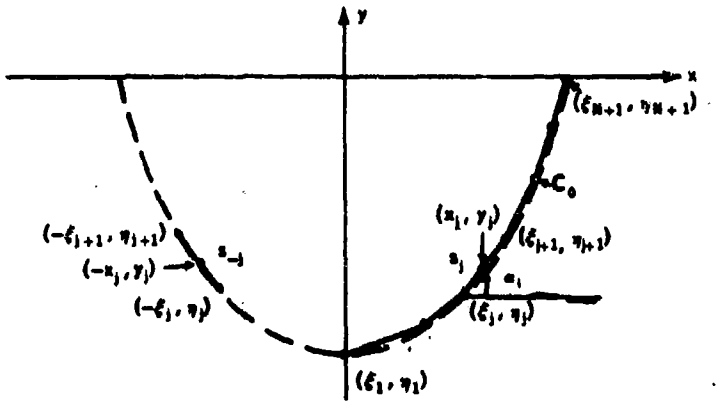

Figure 1 – Polygonal Approximation to Immersed Part of Cylindrical Cross Section C_0

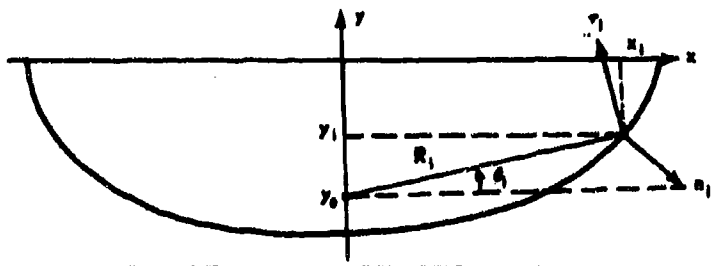

Figure 2 – Kinematics of Roll Oscillation

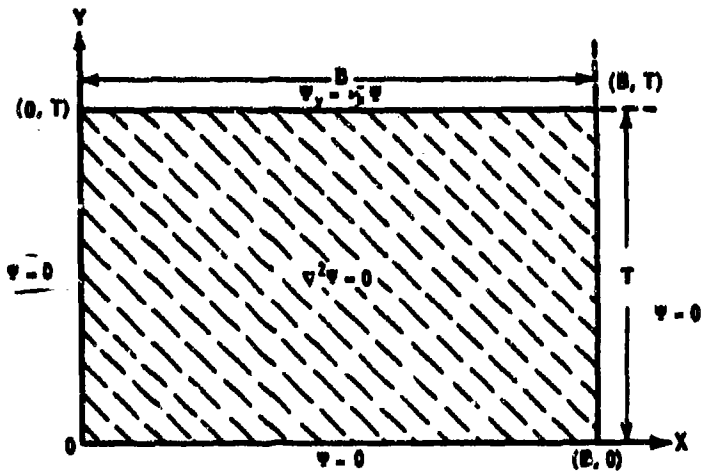

Figure 3 – Adjoint Interior Boundary Value Problem

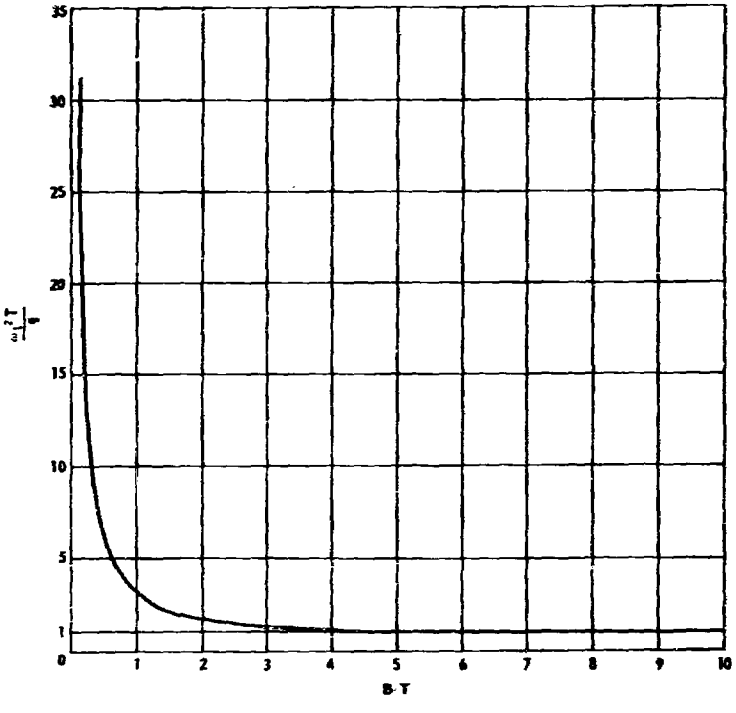

Figure 4 – First Irregular Wave Number as a Function of B/T with T Fixed for Rectangular Cylinders

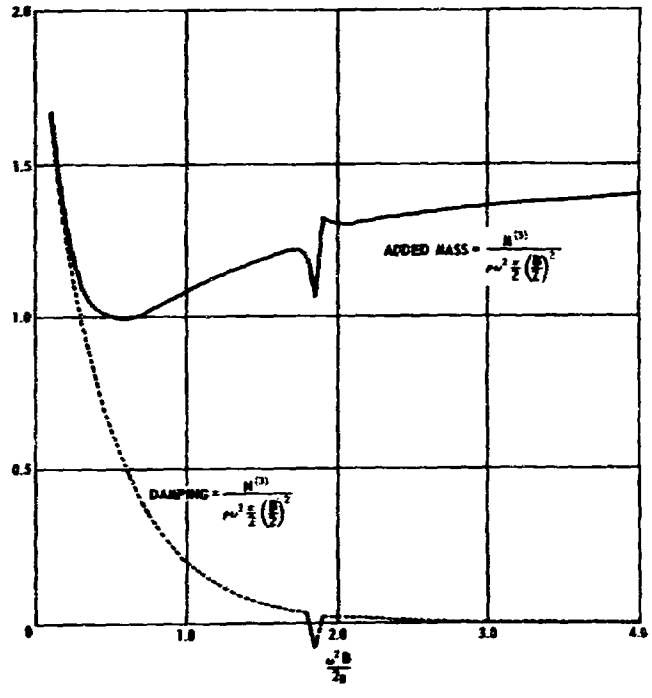

Figure 5 – Heave Added Mass and Damping Coefficients for Rectangular Cylinder

($B/T = 2.5$, 16 Point Input)

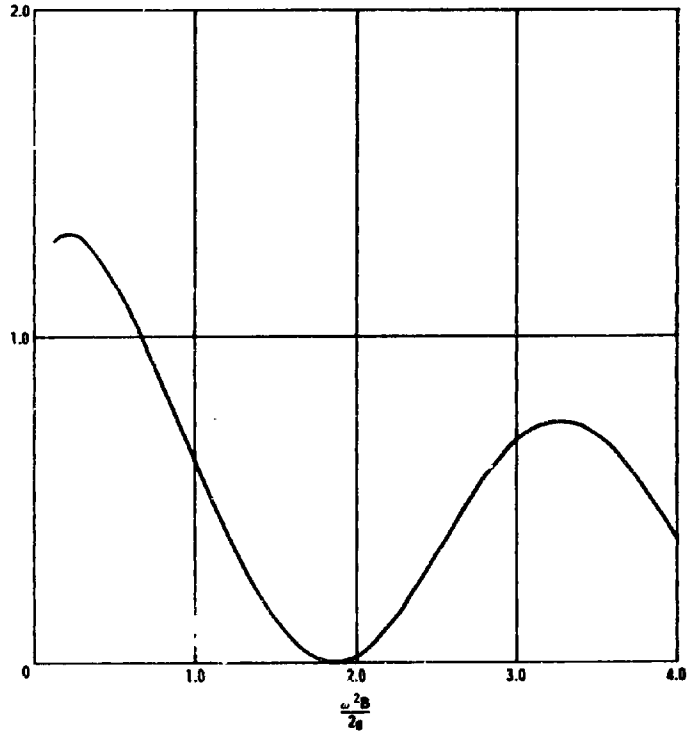

Figure 6 – Scaled Determinant of Matrix of Influence Coefficients for Heaving Rectangular Cylinder

($B/T = 2.5$, 16 Point Input)

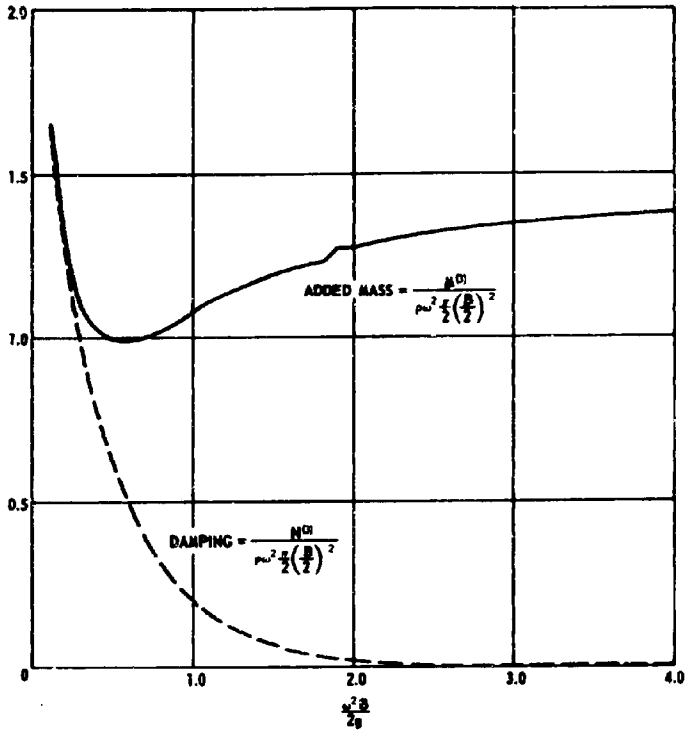

Figure 7 – Heave Added Mass and Damping Coefficients for Rectangular Cylinder

($B/T = 2.5$, 21 Point Input)

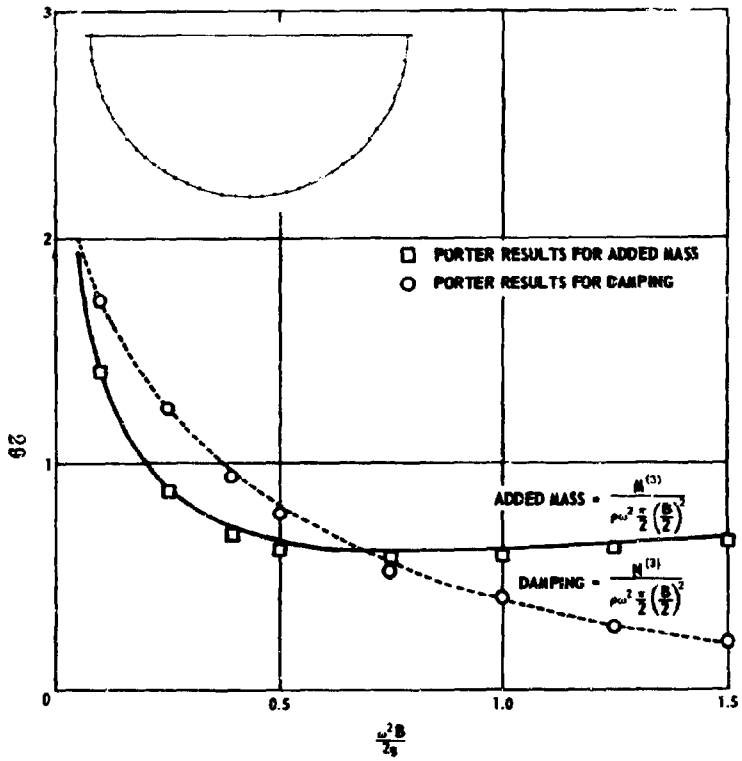

Figure 8 – Heave Added Mass and Damping Coefficients for Semi-Immersed Circular Cylinder

(Defined by 21 Input Points per Half Section)

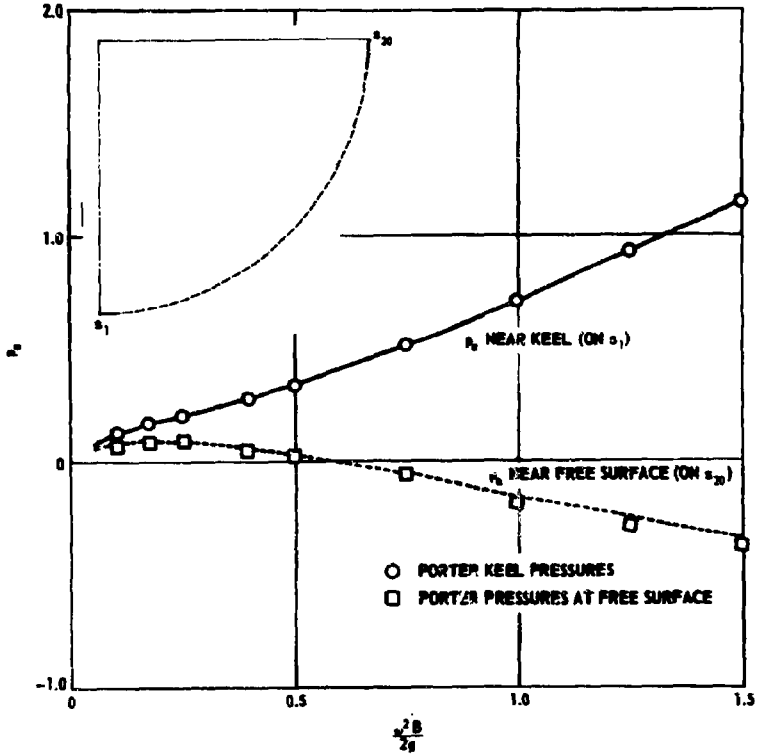

Figure 9 – Pressure in Phase with Displacement on Heaving Semi-Immersed Circular Cylinder

(21 Input Points)

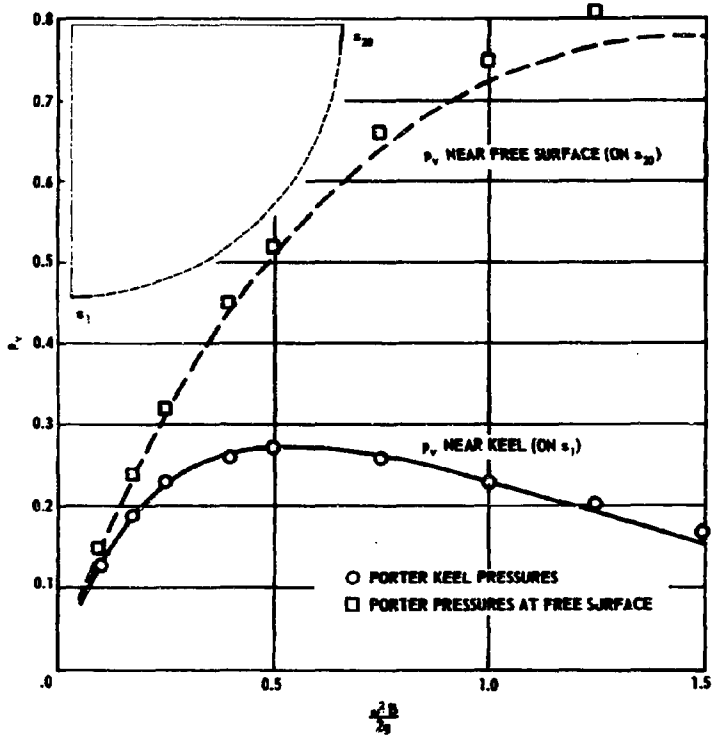

Figure 10 – Pressure in Phase with Velocity on Heaving Semi-Immersed Circular Cylinder

(21 Input Points)

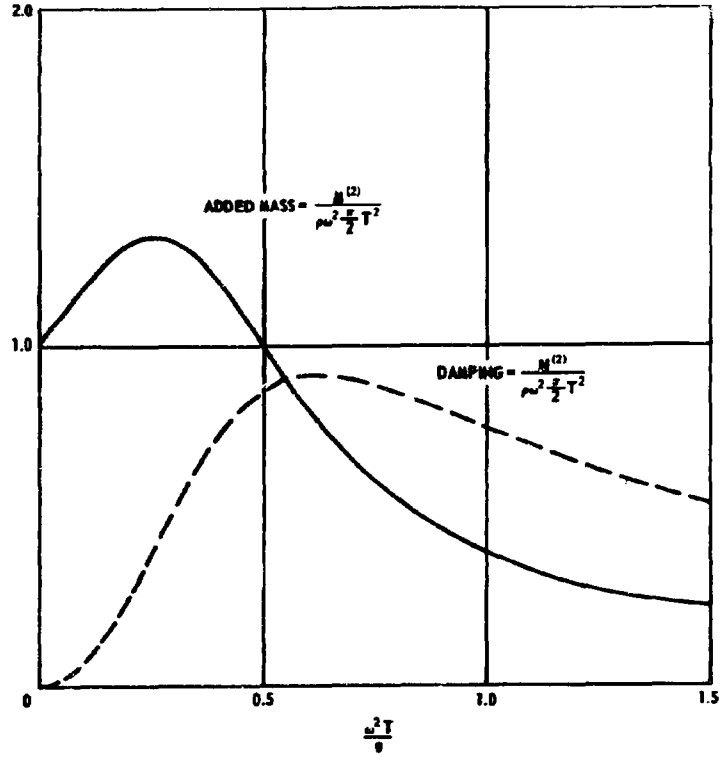

Figure 11 – Sway Added Mass and Damping Coefficients for Semi-Immersed Circular Cylinder

(Defined by 21 Input Points per Half Section)

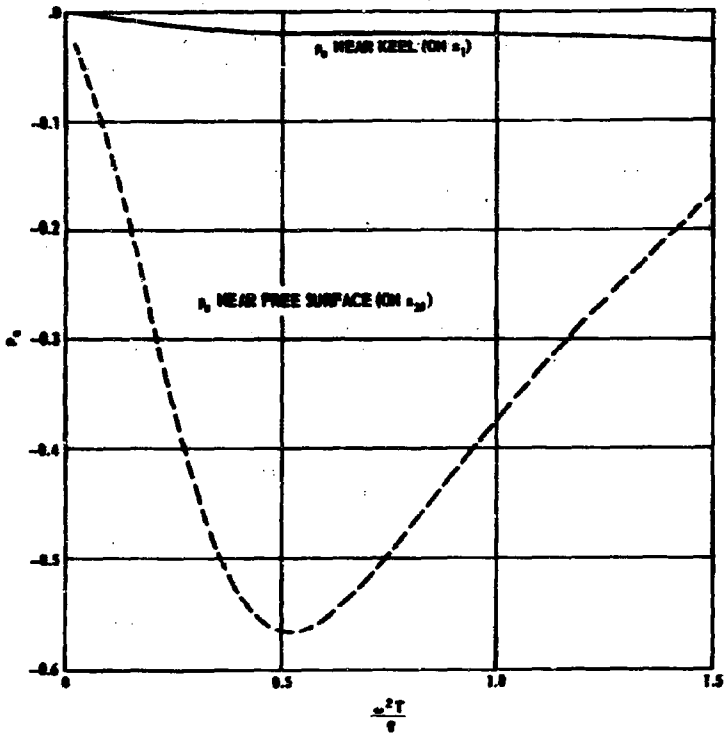

Figure 12 – Pressure in Phase with Displacement on Swaying Semi-Immersed Circular Cylinder

(21 Input Points)

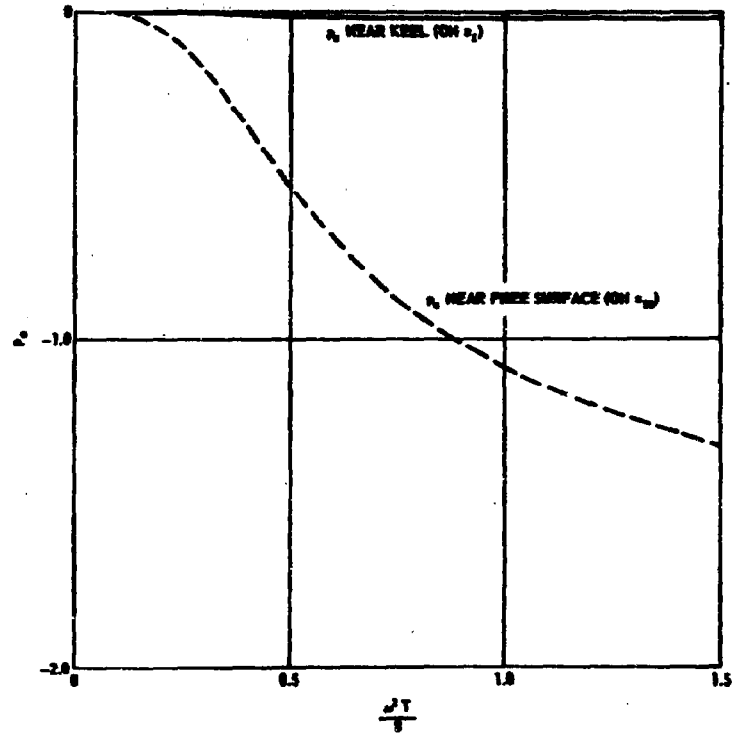

Figure 13 – Pressure in Phase with Velocity on Swaying Semi-Immersed Circular Cylinder

(21 Input Points)

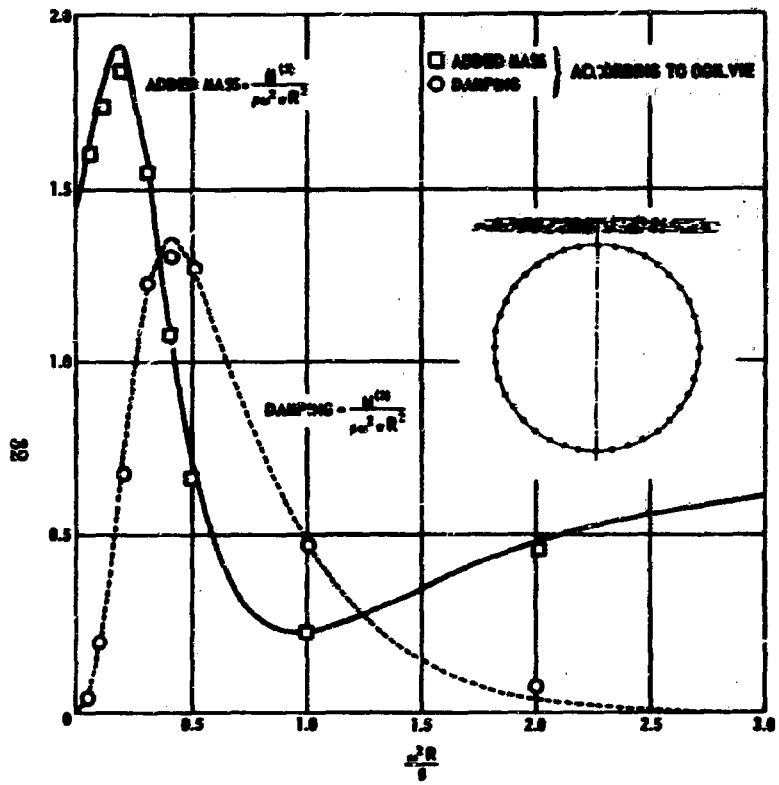

Figure 14 – Added Mass and Damping Coefficients of Fully Submerged Heaving Circular Cylinder

(21 Input Points, Submersion of Axis = 1.25 R)

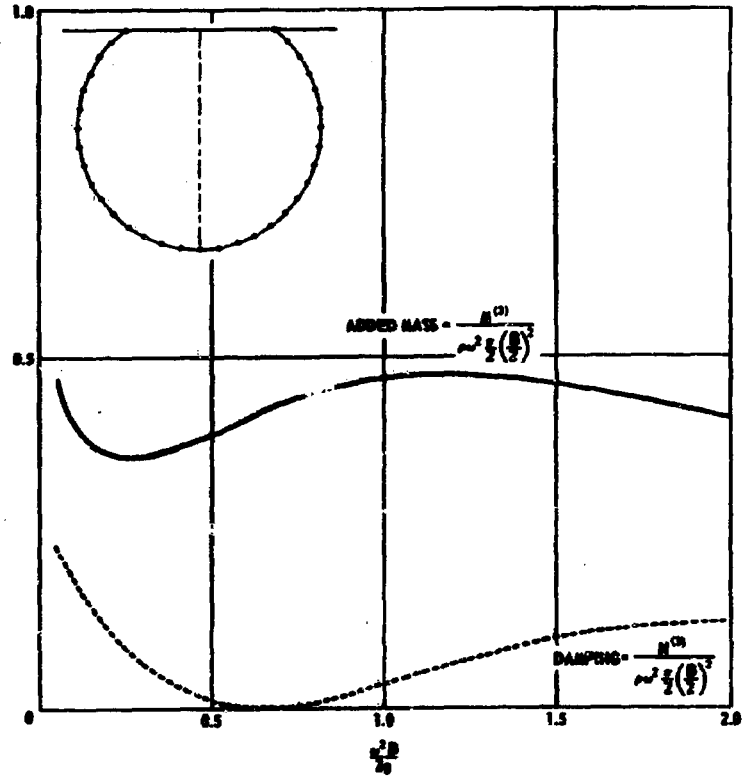

Figure 15 – Added Mass and Damping Coefficients of Heaving Ogival Cylinder

(Draft/Diameter = 9/10, Beam/Diameter = 3/5, 17 Input Points per Half Section)

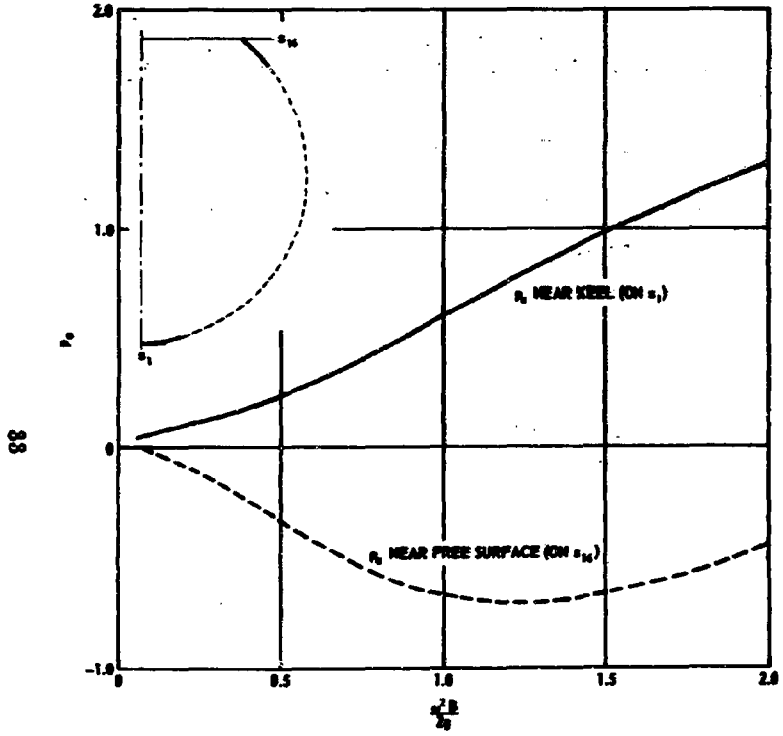

Figure 16 – Pressure in Phase with Displacement on Heaving Ogival Cylinder

($T/D = 9/10$, $B/D = 3/5$, 17 Input Points)

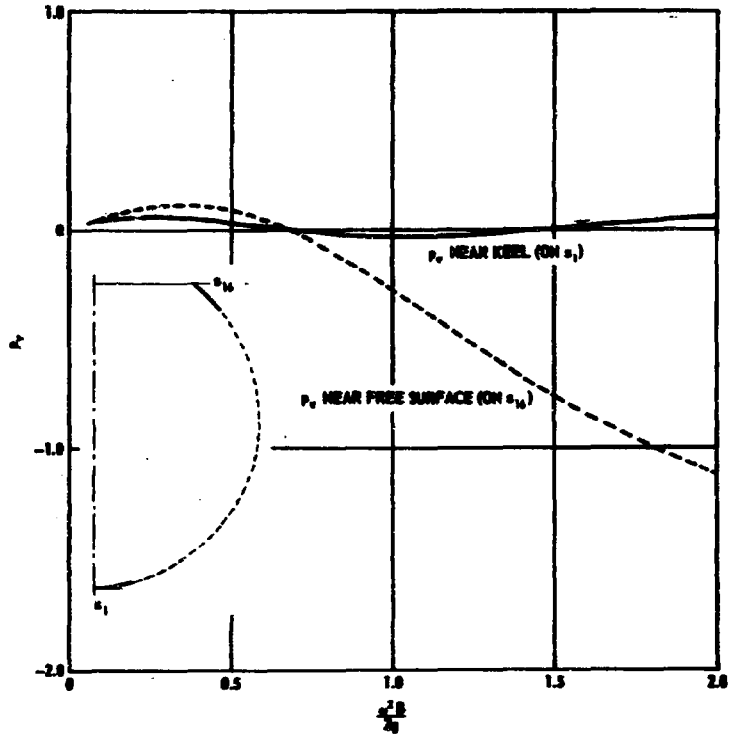

Figure 17 – Pressure in Phase with Velocity on Heaving Ogival Cylinder

($T/D = 9/10$, $B/D = 3/5$, 17 Input Points)

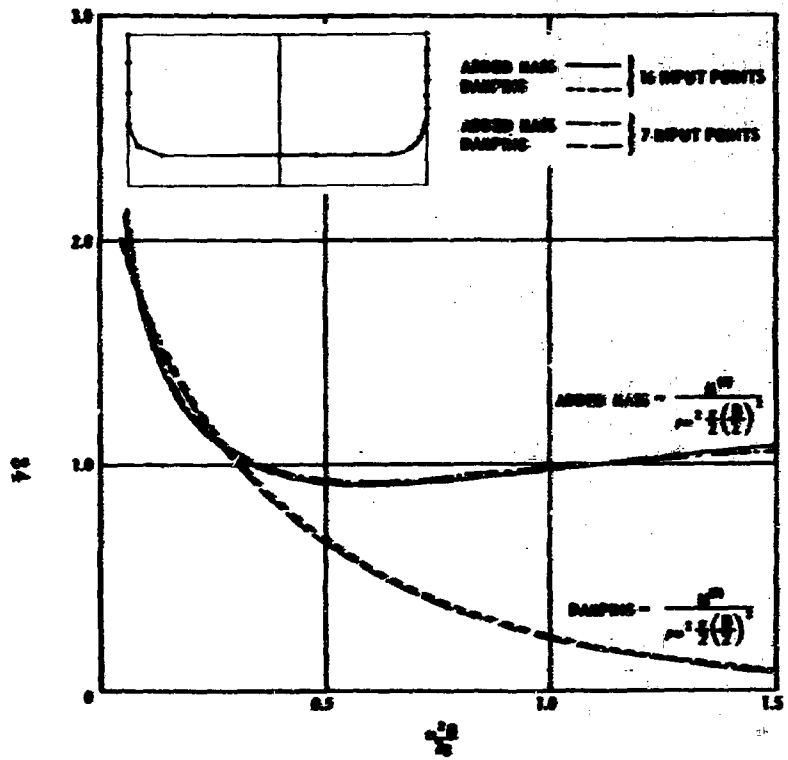

Figure 18 – Heave Added Mass and Damping Coefficients for Midsection of Series 60, Block 70 Ship

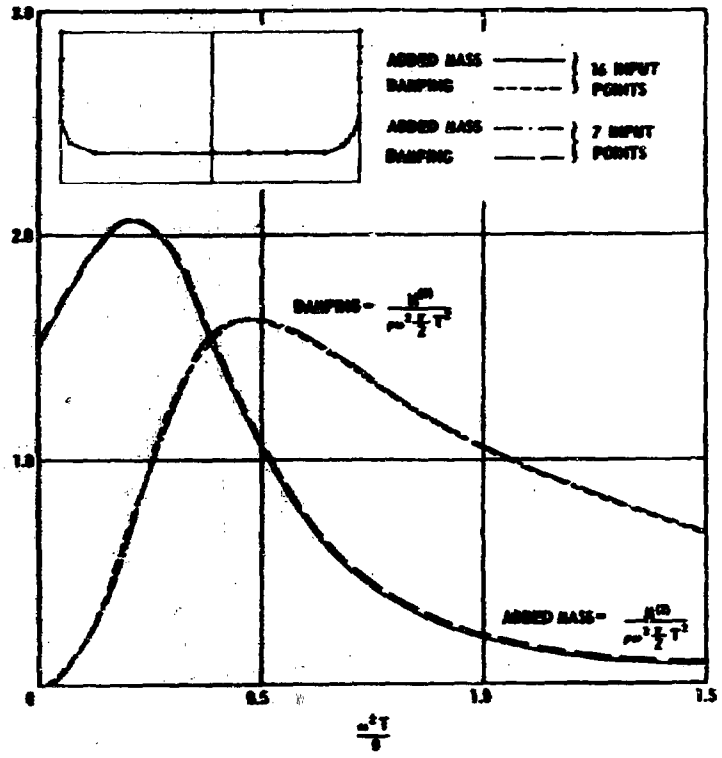

Figure 19 – Sway Added Mass and Damping Coefficients for Midsection of Series 60, Block 70 Ship

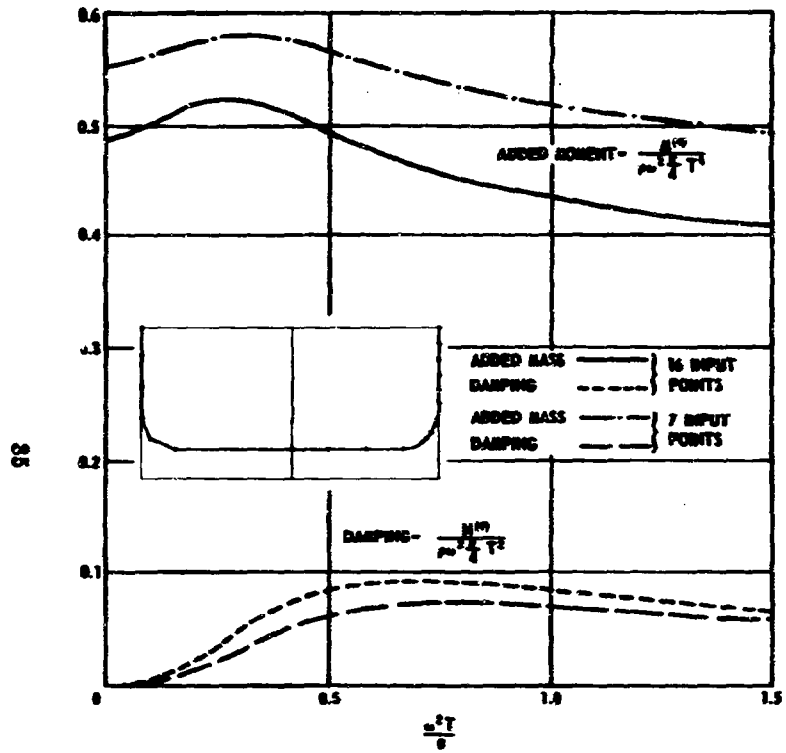

Figure 20 – Roll Added Moment and Damping Coefficients for Midsection of Series 60, Block 70 Ship

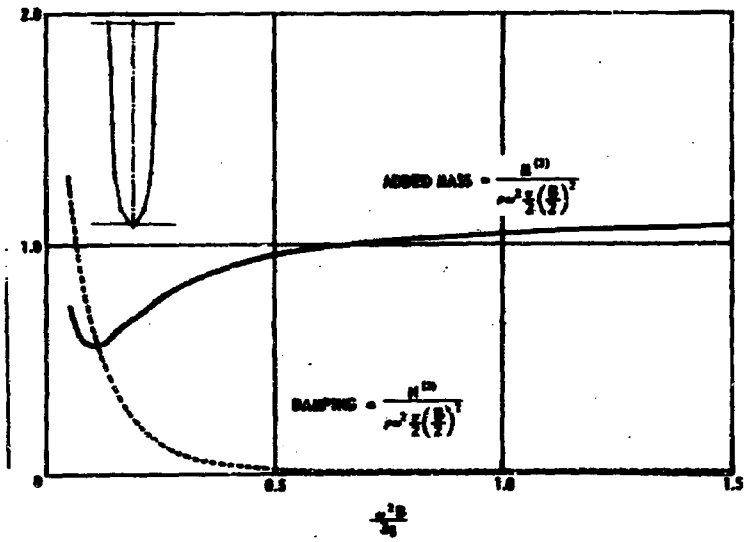

Figure 21 – Heave Added Mass and Damping Coefficients for Bow Section of Series 60, Block 70 Ship

(7 Input Points)

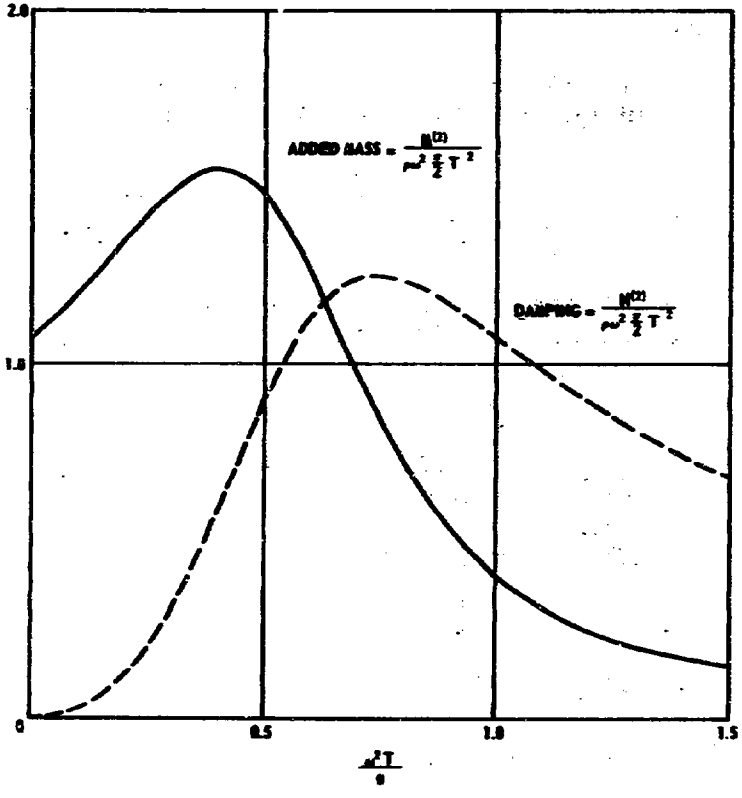

Figure 22 – Sway Added Mass and Damping Coefficients for Bow Section of Series 60, Block 70 Ship

(7 Input Points)

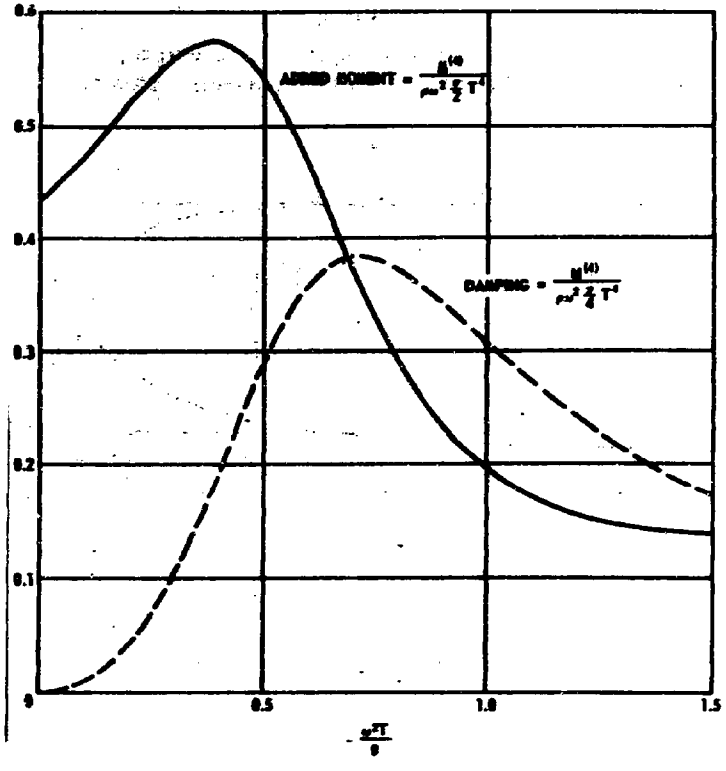

Figure 23 – Roll Added Moment and Damping Coefficients for Bow Section of Series 60, Block 70 Ship

(7 Input Points)

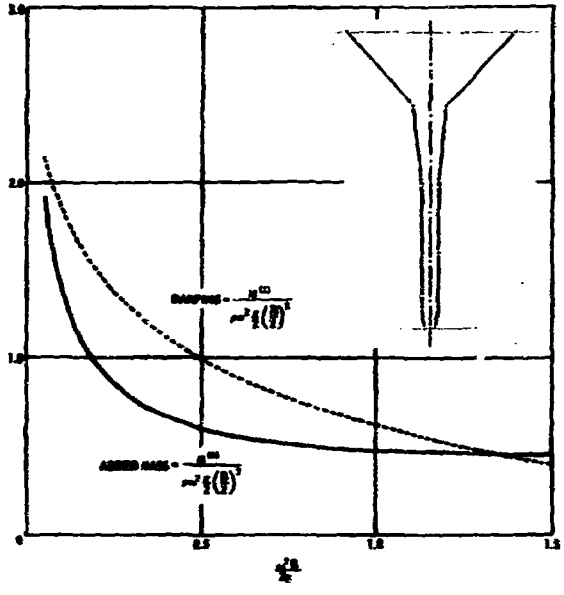

Figure 24 – Heave Added Mass and Damping Coefficients for Aft Section of Series 60, Block 70 Ship

(7 Input Points)

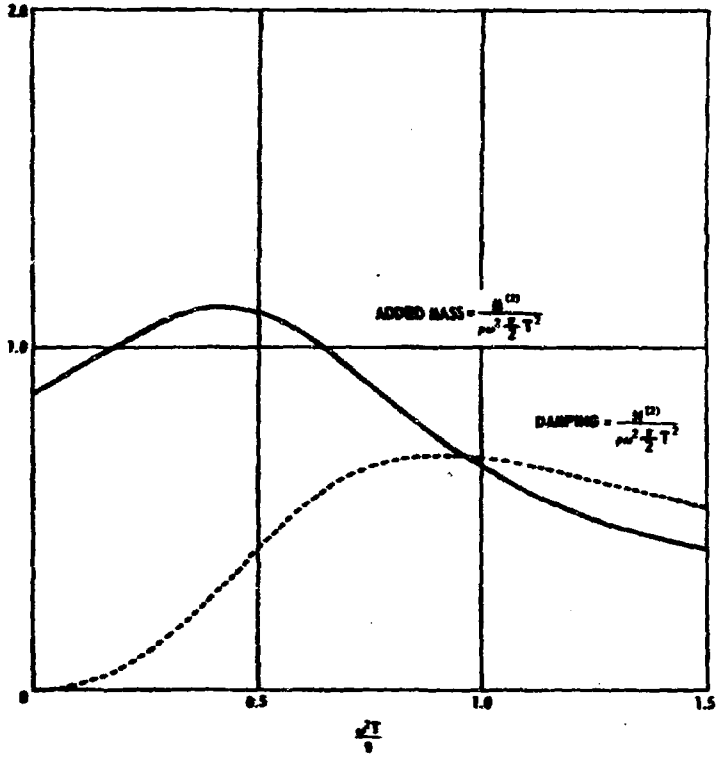

Figure 25 – Sway Added Mass and Damping Coefficients for for Aft Section of Series 60, Block 70 Ship

(7 Input Points)

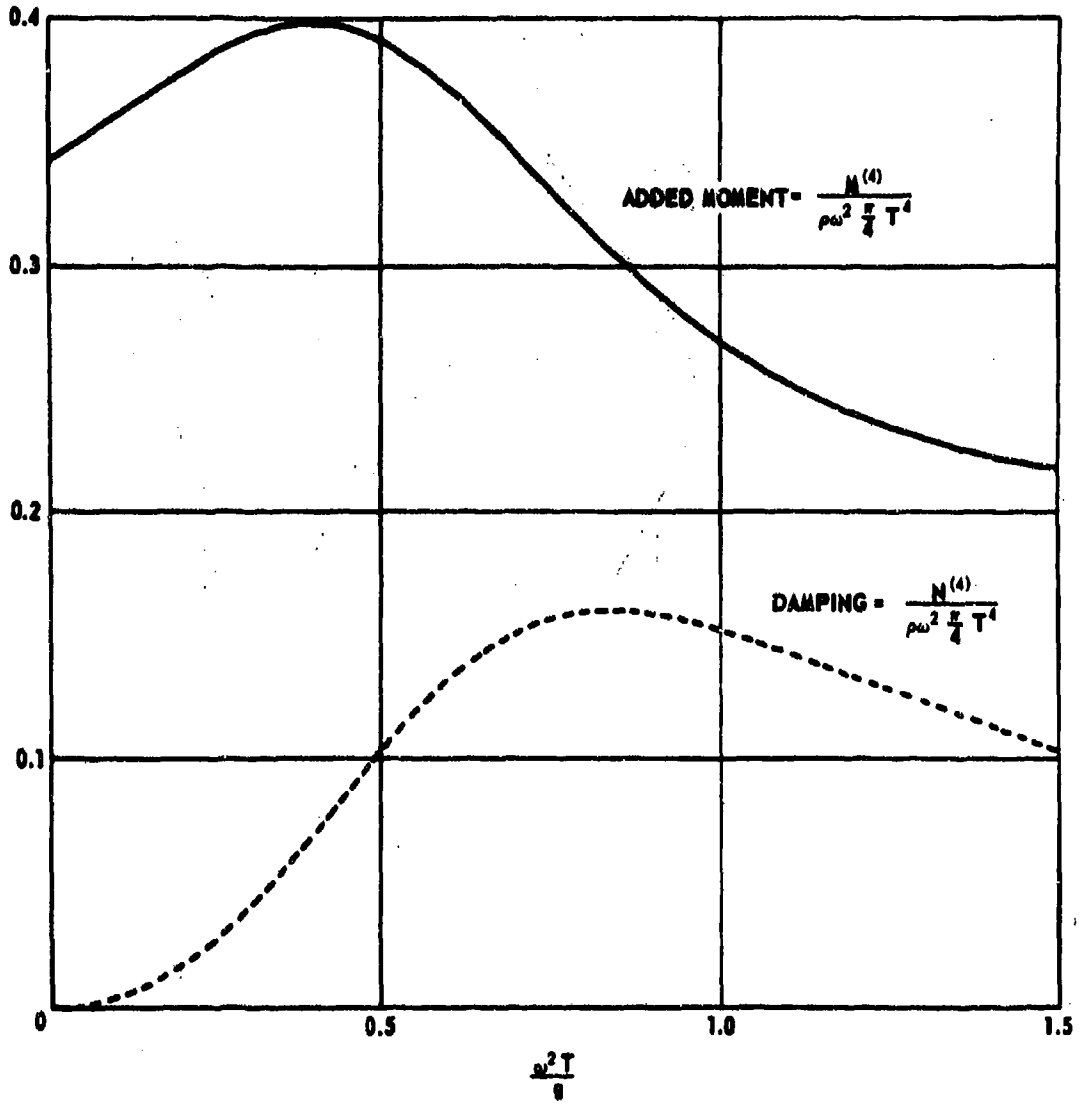

Figure 26 – Roll Added Moment and Damping Coefficients for Aft Section of Series 60, Block 70 Ship

(7 Input Points)

REFERENCES

1. Ursell, F., "On the Heaving Motion of a Circular Cylinder on the Surface of a Fluid," Quarterly Journal of Mechanics and Applied Mathematics, Vol. 2, pp. 218–231 (1949).

2. Grim, O., "Berechnung der durch Schwingungen eines Schiffskoerpers Erzeugten Hydrodynamischen Kraefte," Jahrbuch der Schiffsbautechnischen Gesellschaft, Vol. 47, pp. 277–299 (1953).

3. Tasai, F., "On the Damping Force and Added Mass of Ships Heaving and Pitching," Journal of Zosen Kiokai, Vol. 105, pp. 47–56 (1959).

4. Porter, W.R., "Pressure Distributions, Added Mass, and Damping Coefficients for Cylinders Oscillating in a Free Surface," University of California, Institute of Engineering Research, Report 82-16, Berkeley, California (1960).

5. Ogilvie, T.F., "First and Second Order Forces on a Cylinder Submerged under a Free Surface," Journal of Fluid Mechanics, Vol. 16, Part 3, pp. 451–472 (1963).

6. Korvin-Kroukovsky, B.V., "Investigation of Ship Motions in Regular Waves," Transactions of the Society of Naval Architects and Marine Engineers, Vol. 63, pp. 386–435 (1955).

7. Gerritsma, J., "Distribution of Hydrodynamic Forces Along the Length of a Ship Model in Waves," Shipbuilding Laboratory Publication 144, Technological University, Delft, Netherlands (1966).

8. Smith, W.E., "Computation of Pitch and Heave Motions for Arbitrary Ship Forms," Shipbuilding Laboratory Publication 148, Technological University, Delft, Netherlands (1966).

9. Grim, O., "A Method for a More Precise Computation of Heaving and Pitching Motions Both in Smooth Water and in Waves," Proceedings, Third Symposium on Naval Hydrodynamics, Scheveningen, Netherlands (1960).

10. Vassilopoulos, L., "The Analytical Prediction of Ship Performance in Random Seas," M. I. T. Department of Naval Architecture and Marine Engineering, Cambridge, Mass. (1964).

11. Stoker, J.J., "Water Waves," Interscience Publishers, Inc, New York, (1957).

12. Wehausen, J.V. and Laitone, E.V., "Surface Waves," Handbuch der Physik, (Encyclopedia of Physics), edited by S. Fluegge, Vol. 9, Fluid Dynamics 3, Springer-Verlag, Berlin, Germany, pp. 446–778 (1960).

13. John, F., "On the Motion of Floating Bodies II," Communications on Pure and Applied Mathematics, Vol. 3, Interscience Publishers, Inc, New York, pp. 45–101 (1950).

14. Motora, S. and Koyama, T., "On Wave-Excitation Free Ship Forms," Journal of Zosen Kiokai, Vol. 117 (Jun 1965).

15. Abramowitz, M. and Stegun, I.A., "Handbook of Mathematical Functions with Formulas, Graphs and Mathematical Tables," National Bureau of Standards, U.S. Department of Commerce, Applied Mathematics Series 55 (Jun 1964).

UNCLASSIFIED

Security Classification

DOCUMENT CONTROL DATA - R & D

(Security classification of title, body of abstract and indexing annotation must be entered when the overall report is classified)

1. ORIGINATING ACTIVITY *(Corporate author)*

Naval Ship Research and Development Center
Washington, D.C. 20007

2a. REPORT SECURITY CLASSIFICATION
UNCLASSIFIED

2b. GROUP

3. REPORT TITLE

OSCILLATION OF CYLINDERS IN OR BELOW THE FREE SURFACE OF DEEP FLUIDS

4. DESCRIPTIVE NOTES *(Type of report and inclusive dates)*

5. AUTHOR(S) *(First name, middle initial, last name)*

Frank, Werner

6. REPORT DATE	7a. TOTAL NO. OF PAGES	7b. NO. OF REFS
October 1967	48	15

8a. CONTRACT OR GRANT NO.

b. PROJECT NO. S-R009 01 01
Task 0100

c.

d.

9a. ORIGINATOR'S REPORT NUMBER(S)
2375

9b. OTHER REPORT NO(S) *(Any other numbers that may be assigned this report)*

10. DISTRIBUTION STATEMENT

This document has been approved for public release and sale; its distribution is unlimited.

11. SUPPLEMENTARY NOTES

12. SPONSORING MILITARY ACTIVITY
Naval Ship Research and Development Center

13. ABSTRACT

The subject of cylinders oscillating in or below the free surface of very deep fluids is developed as a boundary value problem within the framework of linear free-surface theory by distributing source singularities over the submerged portion of the cylinders. A computer program for calculating the hydrodynamic pressure, force, and moment of fluids on these cylinders has been devised by the Naval Ship Research and Development Center. The results for various two-dimensional shapes are given in graphical form.

UNCLASSIFIED

Security Classification

14. KEY WORDS	LINK A		LINK B		LINK C	
	ROLE	WT	ROLE	WT	ROLE	WT
Pressures and forces on oscillating cylinders						
Added mass coefficients of cylinders						
Damping coefficients of cylinders						
Two-dimensional water wave problem						

DD FORM 1 NOV 68 1473 (BACK)

(PAGE 2)

GPO 934-234

UNCLASSIFIED

Security Classification